# Broad-Band Two-Dimensional Fourier Transform Ion Cyclotron Resonance

**Peter Pfändler,[†] Geoffrey Bodenhausen,*[†] Jacques Rapin,[‡] Marc-Etienne Walser,[‡] and Tino Gäumann*[‡]**

*Contribution from the Institut de Chimie Organique, Université de Lausanne, Rue de la Barre 2, CH-1005 Lausanne, Switzerland, and Institut de Chimie Physique, Ecole Polytechnique Fédérale, CH-1015 Lausanne, Switzerland.* *Received December 17, 1987*

**Abstract:** Two-dimensional Fourier transform ion cyclotron resonance (2D FT-ICR) allows one to obtain direct evidence for the occurrence of ion–molecule reactions. In 2D FT-ICR spectra, one observes resonances with two distinct frequency coordinates $\omega_1$ and $\omega_2$ that correspond to the mass-to-charge ratios of the ions that participate as reactants and products, respectively. It is possible to monitor a manifold of distinct reactions in one single 2D spectrum. Spectral ranges of the order of several MHz can be covered by using frequency-swept ("chirped") radio-frequency pulses.

Ion cyclotron resonance (ICR) is a remarkably versatile tool for studying gas-phase reactions.[1] With multiple resonance ICR techniques,[2,3] it is possible to eject all ions except for one selected species $A^+$ from the ion-trapping cell and then monitor the recovery of a species $B^+$ due to a reaction of the type $A^+ + C \rightarrow B^+ + D$ (fragmentation, hydrogen or proton transfer, etc.). Such double resonance procedures are closely related to selective perturbation methods in NMR, which tend to be increasingly replaced by two-dimensional (2D) exchange spectroscopy.[4,5] In NMR, the 2D exchange method—which is often referred to as "NOESY" because of applications to the study of nuclear Overhauser effects—has a number of advantages over traditional double-resonance schemes, the most striking advantage being the ability to unravel a manifold of magnetization transfer processes that occur simultaneously.[6] Recently, we have demonstrated that two-dimensional Fourier transform techniques can also be applied to FT-ICR.[7] The resulting two-dimensional spectra show resonances at frequency coordinates $\omega_1$ and $\omega_2$ that correspond to the mass-to-charge ratios of the reactant and product ions respectively.

Normally, 2D methods employ monochromatic radio-frequency pulses that can only cover a limited frequency bandwidth, a limitation that is particularly severe in FT-ICR, though it may also be troublesome in NMR, in ESR[8,9] or in microwave spectroscopy.[10] In one-dimensional FT-ICR, such bandwidth problems can be overcome by using frequency-swept pulses.[11] In this paper, we demonstrate that such "chirped" pulses can also be used in conjunction with two-dimensional spectroscopy, provided suitable precautions are taken to ensure that the radio-frequency phase is varied without discontinuity. In this manner, *broad-band* 2D FT-ICR spectra can be obtained with bandwidths of the order of several megahertz.

The basic sequence of pulses and delays for 2D FT-ICR is shown in Figure 1. The gas under investigation is admitted to the cell at a pressure of the order of $10^{-8}$ mbar. After eliminating all ions that are left over from previous experiments with a quench pulse (electric field across the cell), a pulsed electron beam generates ions in the center of the cell. The essential part of the 2D FT-ICR experiment consists of a sequence of three radio-frequency pulses that are closely analogous to those required for 2D exchange spectroscopy in NMR:

$$P_1 - t_1 - P_2 - \tau_m - P_3 - t_2 \qquad (1)$$

where we distinguish the *evolution interval* $t_1$, the *reaction* or *mixing period* $\tau_m$, and the *detection interval* $t_2$. The symbols $P_1$, $P_2$, and $P_3$ represent the three radio-frequency pulses. We shall begin by discussing the basic single-frequency 2D FT-ICR experiment, where all three pulses are derived from a single continuously running monochromatic frequency source $\omega^{rf}$. In this case, it is convenient to discuss the phases of the ion packets and rf pulses in a rotating frame synchronized with the transmitter carrier frequency $\omega^{rf}$, a procedure that may be applied to both FT-ICR and NMR. The first rf pulse $P_1$ in the sequence of eq 1, acting on trapped but incoherent ions, excites the ion packets coherently onto cyclotron trajectories. The ions, which have initially a low kinetic energy that corresponds to the ambient temperature, are heated up in this process. In the evolution time $t_1$, the coherent packet of an arbitrary species of ions $A^+$ precesses at an offset $\Delta\omega^A = \omega^A - \omega^{rf}$ with respect to the carrier frequency. The decay due to the loss of phase coherence in the course of the evolution time $t_1$ is negligible ($t_1^{max}$ is of the order of 250 $\mu$s in our experiments). The coherent packet of ions accumulates a phase difference $\Delta\varphi^A = \Delta\omega^A t_1$ with respect to the carrier phase. Provided this relative phase is $(2k + 1)\pi$ (with $k = 0, 1, \ldots$) at the end of $t_1$, the second rf pulse $P_2$ leads to "de-excitation" of the ion packet.[12] In this case, the ions "spiral inward" on an orbit with decreasing radius, so that they are cooled down. If the phase-difference $\Delta\varphi^A$ differs from $(2k + 1)\pi$, however, the ions are not cooled down completely; in fact, some are actually accelerated onto higher orbits by the second rf pulse. In the subsequent reaction interval $\tau_m$ (typically 300 ms), the hot ions lose their phase coherence with a time constant which in our experiments is of the order of 40 ms. On the other hand, the number of "cold" ions $A^+$ that have been properly de-excited at the beginning of the $\tau_m$ interval is obviously modulated as a function of $\Delta\omega^A t_1$. These cold ions can be observed in the usual manner after the detection pulse $P_3$, which leads to a signal that is approximately proportional to $[a_0 - a_1 \cos \Delta\omega^A t_1]$. The $t_1$ modulation is essentially cosinusoidal provided the amplitudes of the pulses $P_1$ and $P_2$ are chosen such that the radius of the orbiting ions in the $t_1$ interval is of the order of 20–50% of the optimum radius that is compatible with the dimensions of the cavity. If the pulse amplitude is too large, the $t_1$ modulation is no longer simply cosinusoidal but acquires the character of a shah function,[7] leading to harmonic signals in the $\omega_1$ domain. These $\omega_1$ harmonics have

[†] Université de Lausanne.
[‡] Ecole Polytechnique Fédérale.

(1) Marshall, A. G. *Acc. Chem. Res.* **1985**, *18*, 316.
(2) Anders, L. R.; Beauchamp, J. L.; Dunbar, R. C.; Baldeschwieler, J. D. *J. Chem. Phys.* **1966**, *45*, 1062.
(3) Comisarow, M. B.; Grassi, V.; Parisod, G. *Chem. Phys. Lett.* **1978**, *57*, 413.
(4) Meier, B. H.; Ernst, R. R. *J. Am. Chem. Soc.* **1979**, *101*, 6441.
(5) Jeener, J.; Meier, B. H.; Bachmann, P.; Ernst, R. R. *J. Chem. Phys.* **1979**, *71*, 4546.
(6) Ernst, R. R.; Bodenhausen, G.; Wokaun, A. *Principles of Nuclear Magnetic Resonance in One and Two Dimensions*; Clarendon: Oxford, 1987.
(7) Pfändler, P.; Bodenhausen, G.; Rapin, J.; Houriet, R.; Gäumann, T. *Chem. Phys. Lett.* **1987**, *138*, 195.
(8) Gorcester, J.; Freed, J. H. *J. Chem. Phys.* **1986**, *85*, 5375.
(9) Höfer, P.; Grupp, A.; Nebenführ, H.; Mehring, M. *Chem. Phys. Lett.* **1986**, *132*, 279.
(10) Vogelsanger, B.; Andrist, M.; Bauder, A. *Chem. Phys. Lett.* **1988**, *144*, 180.
(11) Comisarow, M. B.; Marshall, A. G. *Chem. Phys. Lett.* **1974**, *26*, 489.
(12) Marshall, A. G.; Wang, T.-C. L.; Ricca, T. L. *Chem. Phys. Lett.* **1984**, *105*, 233.

0002-7863/88/1510-5625$01.50/0 

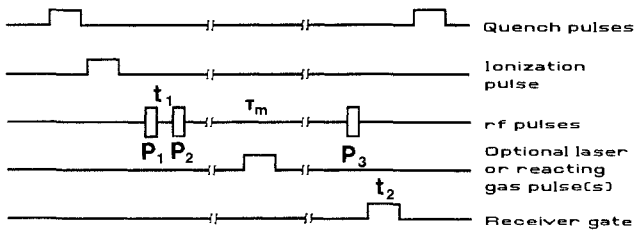


**Figure 1.** Basic sequence of pulses and delays for 2D FT-ICR, with quench pulses, ionization pulse, and three radio-frequency (rf) pulses $P_1$, $P_2$, and $P_3$, separated by the evolution time $t_1$ and the reaction interval $\tau_m$. In the basic monochromatic (narrow-band) experiment, all three rf pulses are derived from a continuously running frequency generator, while in the broad-band experiment they are swept through the relevant range of frequencies ("chirped"). In the reaction interval $\tau_m$, one may apply a laser pulse to induce photodissociation or introduce a pulse of reacting gas to monitor the effects of ion–molecule collisions.

a different physical origin from the harmonics observed in conventional one-dimensional ICR spectra,[13] which in our experiments would lead to rows of signals at distinct frequencies in the $\omega_2$ domain.

In the reaction interval $\tau_m$, a variety of processes may occur, such as reactions of the type $A^+ + C \rightarrow B^+ + D$. These could be ion–molecule reactions, but C may also be a photon capable of inducing photofragmentation. One may contemplate other perturbations to be inflicted on the ions in the course of the reaction interval $\tau_m$; for example, the ions $A^+$ might be re-excited by an additional rf pulse to study collision-induced fragmentation. Since the number of $A^+$ ions at the beginning of $\tau_m$ is modulated by $\cos \Delta\omega^A t_1$, the number of $B^+$ ions that result from the reaction $A^+ + C \rightarrow B^+ + D$ must also be modulated by the same function. Thus the number of incoherent $B^+$ ions at the end of $\tau_m$ is modulated by the frequency offset $\Delta\omega^A$ of the *precursor* $A^+$ in the reaction. A time-domain signal $s(t_1, t_2)$ is observed in the detection period $t_2$ for systematic increments of $t_1$, and a 2D spectrum $S(\omega_1,\omega_2)$ is obtained by two-dimensional Fourier transformation.[6] The occurrence of a "cross-peak" at frequency coordinates $\omega_1 = \Delta\omega^A$ and $\omega_2 = \Delta\omega^B$ (offsets with respect to the monochromatic carrier frequency) provides definite evidence for a reaction $A^+ + C \rightarrow B^+ + D$.

If the 2D experiment is carried out in this manner with monochromatic pulses, the applications are rather limited, for only narrow frequency bandwidths can be covered.[7] This is why it is necessary to design a broad-band version of the 2D technique. In *chirped-frequency* 2D FT-ICR, the rf frequency of each of the three pulses in the sequence of eq 1 is rapidly swept through the relevant range of frequencies. In our experiments, which have been carried out on a Spectrospin CMS-47 ICR spectrometer, each pulse of total duration $\tau_p = N\tau_i$ starts with the highest frequency $\omega_1^{rf}$, which is then decremented through $N$ discrete steps with decreasing frequencies $\omega_1^{rf} \ldots \omega_N^{rf}$ in the $N$ consecutive intervals $\tau_i$. This is shown schematically in Figure 2, where it has been assumed for clarity that each radio-frequency pulse consists of only three intervals $\tau_1$, $\tau_2$, $\tau_3$ with three different frequencies $\omega_1^{rf}$, $\omega_2^{rf}$, $\omega_3^{rf}$. As the frequency is decremented, the phase varies without discontinuity, as shown in Figure 2. This feature is essential to the success of the experiment. Let the rf phase (in the laboratory system) at the beginning of the first pulse be called $\varphi_0^{rf}$. The rf phase at the end of the $n$th interval $\tau_n$ is then

$$\varphi_n^{rf} = \varphi_0^{rf} + \sum_{i=1}^{n} \omega_i^{rf} \tau_i \qquad (2)$$

Now we may assume for simplicity that a packet of ions $A_n^+$ is only affected by the rf irradiation in the $n$th interval $\tau_n$, i.e. we assume that the frequencies $\omega_1^{rf} \ldots \omega_{n-1}^{rf}$ and $\omega_{n+1}^{rf} \ldots \omega_N^{rf}$ are too far off-resonance to influence the motion of these ions. In this case, the phase $\varphi_n^A$ of the coherent packet of ions $A_n^+$ at the end

(13) Nikolaev, E. N.; Gorshkov, M. V. *Int. J. Mass Spectrom. Ion Processes* **1985**, *64*, 115.

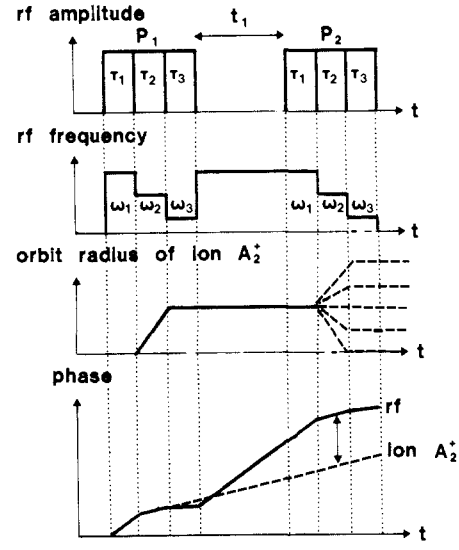


**Figure 2.** Excitation and "de-excitation" by the first two rf pulses of the broad-band 2D FT-ICR sequence. For the sake of illustration, each chirped pulse is broken down into only three consecutive intervals, $\tau_1$, $\tau_2$, $\tau_3$, where the rf frequency is stepped down through $\omega_1^{rf}$, $\omega_2^{rf}$, $\omega_3^{rf}$. The rf carrier is switched back to the initial (highest) frequency at the beginning of the evolution period $t_1$. The rf phase is varied without discontinuity (solid line in lowest graph). A species $A_2^+$, so-labeled because it is assumed to be resonant with $\omega_2^{rf}$, is not affected by irradiation in the $\tau_1$ and $\tau_3$ intervals. The ion packet "spirals out" during the $\tau_2$ interval of the first pulse (increasing orbit radius), and may "spiral in" again in the $\tau_2$ interval of the second rf pulse, provided the phase of the ion packet (dashed line in lowest graph) is opposite to the rf phase at that time. This phase lag is represented by a double-pointed vertical arrow.

of the $n$th interval is determined only by the rf phase at this time: $\varphi_n^A = \varphi_n^{rf}$. (In actual fact, a constant term may have to be included to account for a possible phase lag.) The ions $A_n^+$ fail to "see" the remaining $(N - n)$ intervals of the first rf pulse, as well as the first $(n - 1)$ intervals of the second pulse. The ions $A_n^+$ simply precess at their characteristic frequency $\omega_n^A$ during these intervals and throughout the evolution period $t_1$. At the beginning of the $n$th interval $\tau_n$ in the second burst, the ions $A_n^+$ will have a phase

$$\varphi_{n-1}^A = \varphi_0^{rf} + \sum_{i=1}^{n} \omega_i^{rf} \tau_i + [(N - 1)\tau_i + t_1]\omega_n^A \qquad (3)$$

The dashed line in the lowest graph of Figure 2 represents the phase of the ions $A_n^+$ (with $n = 2$ in this example). The crucial step in the experiment is the de-excitation of the $A_n^+$ ions by the second pulse. Like in the monochromatic experiment discussed above, this can only occur completely if there is a phase difference of $(2k + 1)\pi$ (with $k = 0, 1, \ldots$) between the phase of the ions and the phase of the rf irradiation at the beginning of the $n$th interval $\tau_n$ in the second burst. This phase difference, which is indicated by a vertical two-pointed arrow in Figure 2, depends on the procedure used for sweeping the frequency of the rf carrier. If at the beginning of the evolution period $t_1$ the rf carrier is reset to the initial (highest) frequency $\omega_1^{rf}$ (see Figure 2), the rf phase at the beginning of the $n$th interval $\tau_n$ in the second pulse will be

$$\varphi_{n-1}^{rf} = \varphi_0^{rf} + \sum_{i=1}^{N} \omega_i^{rf} \tau_i + \omega_1^{rf} t_1 + \sum_{i=1}^{n-1} \omega_i^{rf} \tau_i \qquad (4)$$

The relative phase of the coherent ions $A_n^+$ and the rf irradiation at the beginning of the $\tau_n$ interval in the second burst is therefore

$$\varphi_{n-1}^A - \varphi_{n-1}^{rf} = [\omega_n^A - \omega_1^{rf}]t_1 + \Delta\varphi \qquad (5)$$

where

$$\Delta\varphi = (N - 1)\tau_i \omega_n^A - \sum_{i=1}^{N} \omega_i^{rf} \tau_i + \omega_n^{rf} \tau_n$$

Thus the relative phase is $t_1$ modulated as a function of the offset $[\omega_n^A - \omega_1^{rf}]$ between the frequency of the ions and the frequency

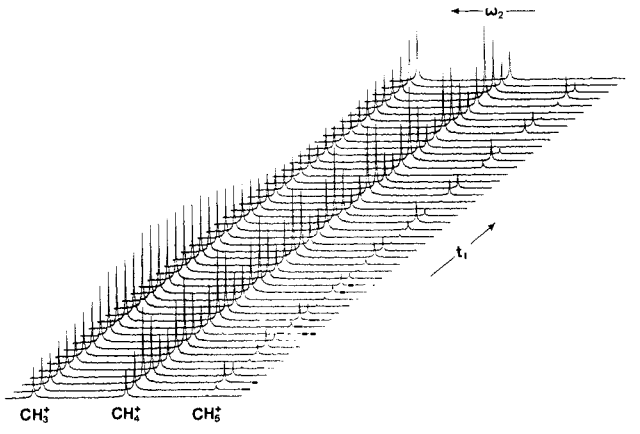


**Figure 3.** Broad-band 2D FT-ICR spectra $S(t_1,\omega_2)$ of methane $CH_4$, shown in absolute value mode prior to Fourier transformation with respect to $t_1$. The reaction interval $\tau_m$ was 500 ms. The evolution time $t_1$ was incremented in 120 steps of 1 μs, with 1K data points recorded in $t_2$. The light primary ion $CH_3^+$ features a slow $t_1$ modulation, because its high cyclotron frequency is near to the initial rf frequency of the chirped pulses.

of the rf source in the $t_1$ period. In our experiments, this rf frequency corresponds to the initial (highest) frequency of the chirp. The remaining constant terms in eq 5 do not influence the frequencies in the spectrum but merely affect the phases of the signals. These phase terms are not relevant in our broad-band 2D experiments since we use absolute value representations.[6]

If the relative phase of eq 5 is an odd multiple of $\pi$, the ions will spiral inward during the $\tau_n$ interval of the second rf pulse and will be robbed of most of their kinetic energy, just as in the monochromatic 2D experiment. The population of the resulting "cold" $A^+$ ions is therefore modulated by $[\omega_n{}^A - \omega_1{}^{rf}]t_1$. If both pulses $P_1$ and $P_2$ are relatively weak, so that the radius of the trajectory in $t_1$ is about 20–50% of the optimum radius, the modulation is again found to be approximately cosinusoidal. The use of relatively weak rf pulses makes it possible to avoid the appearance of signals at harmonic frequencies in the $\omega_1$ domain of the 2D spectrum.[7] Note that in practice the rf field experienced by the ions in the cell is a function of their cyclotron radius.[14] After ion–molecule collisions, fragmentation, or photodissociation according to the scheme $A^+ + C \rightarrow B^+ + D$, the resulting product ions $B^+$ are re-excited in the usual manner by the third pulse in the sequence of eq 1. Normally, the third pulse is also chirped, and the signal is observed in the $t_2$ period without heterodyne detection, so that the frequencies in the $\omega_2$ domain correspond to the true (laboratory frame) cyclotron frequencies rather than to the offset with respect to an rf carrier frequency. The signal of an ion $B^+$, observed at $\omega_2 = \omega^B$, is modulated by the offset $[\omega^A - \omega_1{}^{rf}]$ of its precursor $A^+$, and cross-peaks appear if a reaction has taken place.

To illustrate the potential of 2D FT-ICR, we have chosen two very simple cases, both involving methane. This choice was suggested by the fact that, because of the inverse proportionality of cyclotron frequencies and mass-to-charge ratios, the demands on the bandwidth are greatest if one considers a mixture of light ions such as $CH_3^+$ and ions that have more than twice the mass such as $C_2D_5^+$.

Figure 3 shows a mixed time/frequency domain representation of broad-band 2D FT-ICR spectra of methane. Ionization produces only the two primary ions $CH_3^+$ and $CH_4^{\bullet+}$. One also observes secondary ions $CH_5^+$, but these signals are modulated as a function of $t_1$ at the same frequency as the $CH_4^{\bullet+}$ signals, providing evidence that the secondary $CH_5^+$ ions are daughters of the primary ions $CH_4^{\bullet+}$.

This relationship may be appreciated much more readily after Fourier transformation with respect to $t_1$. The two-dimensional broad-band FT-ICR spectrum $S(\omega_1,\omega_2)$ of methane, derived from the data of Figure 3, is shown in Figure 4. The species $CH_3^+$ and $CH_4^{\bullet+}$ lead to peaks on the *line of primary ions*. These signals correspond to *diagonal peaks* in NMR spectra. The existence of a *cross-peak* to the right of the spectrum (with frequency coordinates $\omega_1$ and $\omega_2$ corresponding to $CH_4^{\bullet+}$ and $CH_5^+$, respectively) provides direct evidence of the occurrence of the ion–molecule reaction $CH_4^{\bullet+} + CH_4 \rightarrow CH_5^+ + CH_3^{\bullet}$. The weak cross-peak to the left of the spectrum is indicative of the reaction $CH_4^{\bullet+} + CH_4 \rightarrow CH_3^+ + H^{\bullet} + CH_4$. Two weak signals in the upper part of the spectrum correspond to harmonics, due to the fact that the rf pulses used in this experiment were somewhat too strong to be within the range of pure cosinusoidal modulation. Note that the $\omega_2$ frequencies (actual cyclotron frequencies in the laboratory frame) are inversely proportional to the mass-to-charge ratios, while the $\omega_1$ frequencies correspond to offsets of the cyclotron frequencies with respect to the initial (highest) frequency used in the chirped pulses. Because of this peculiar situation, it would be awkward to speak of a "diagonal" rather than of a line of primary ions.

Figure 5 shows a broadband 2D FT-ICR spectrum of deuteriated methane $CHD_3$. Like in Figure 4, species with increasing

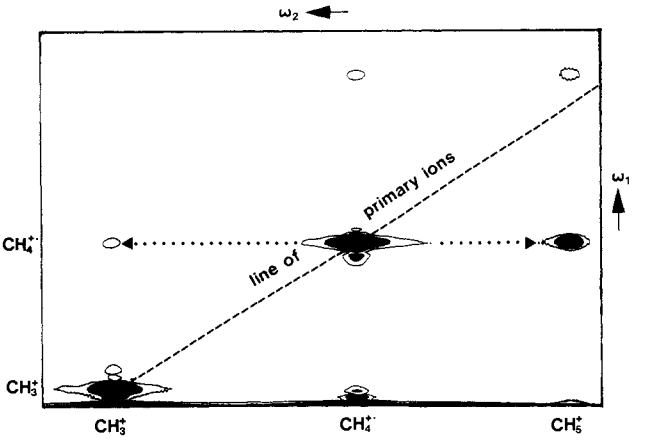


**Figure 4.** Two-dimensional broad-band FT-ICR spectrum $S(\omega_1,\omega_2)$ of methane $CH_4$, derived from the data shown in part in Figure 3. The matrix of 120 × 1K was extended to 256 × 2K by zero-filling prior to Fourier transformation. The spectrum is shown in absolute value mode. Higher contours have been filled in to enhance contrast. The dashed line of primary ions features resonances due to $CH_3^+$ and $CH_4^{\bullet+}$, analogous to diagonal peaks in 2D NMR. The dotted lines indicate how the modulation of the primary ion $CH_4^{\bullet+}$ is transferred to the daughter ions $CH_3^+$ and $CH_5^+$, as evidenced by two cross-peaks emphasized by arrows.

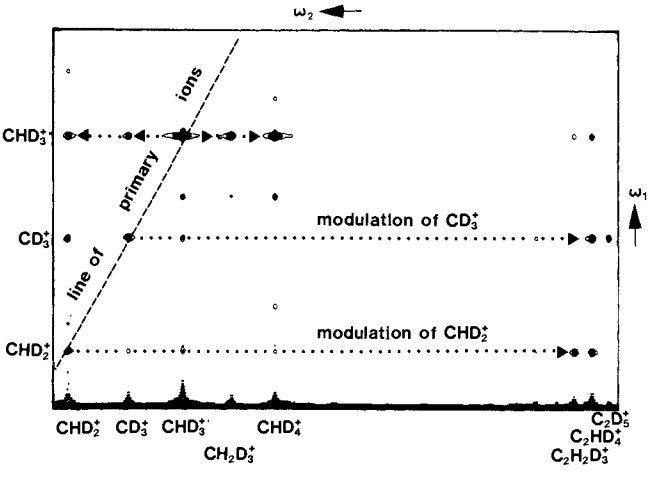


**Figure 5.** Two-dimensional broad-band FT-ICR spectrum $S(\omega_1,\omega_2)$ of partially deuteriated methane $CHD_3$, presented in the same way as Figure 4. The reaction interval $\tau_m$ was 300 ms. The evolution time $t_1$ was incremented in 256 steps of 1 μs, with 1 K data points recorded in $t_2$. The matrix of 256 × 1K was extended to 512 × 2K by zero-filling prior to Fourier transformation. At least eight distinct ion–molecule reactions can be observed in this spectrum, as discussed in the text.

(14) Huang, S. K.; Rempel, D. L.; Gross, M. L. *Int. J. Mass Spectrom. Ion Processes* **1986**, *72*, 15.

mass-to-charge ratios appear from left to right (decreasing cyclotron frequencies $\omega_2$). As may be expected, only the ions $CHD_2^+$, $CD_3^+$, and $CHD_3^{\bullet+}$ give rise to signals on the line of primary ions. Dotted lines with arrows indicate how the $t_1$ modulation ($\omega_1$ frequency) is carried from the primary ions to the secondary ions. The ions $CH_2D_3^+$ and $CHD_4^+$ appear only as daughters of $CHD_3^{\bullet+}$. The heavier ions $C_2HD_4^+$ are produced from collisions involving either $CHD_2^+$ or $CD_3^+$. The species $C_2H_2D_3^+$ only appears as daughter of $CHD_2^+$, while $C_2D_5^+$ stems only from $CD_3^+$. All these processes can be evaluated from a single 2D spectrum.

### Further Experiments

Two-dimensional FT-ICR can be combined with a variety of perturbations. In particular, it is possible to admit a pulse of a neutral reacting gas to the cell in the course of the reaction interval $\tau_m$ of the 2D FT-ICR sequence. A preliminary experiment has shown that this is indeed feasible. The first two rf pulses were applied while the cell contained only argon ions $Ar^+$. In the reaction interval $\tau_m$, a pulse of $CH_4$ gas was introduced into the cell. No further ionization pulses were applied however. In the 2D spectrum, clear evidence was found for secondary ions $CH_3^+$ and even for tertiary ions $C_2H_5^+$, both $t_1$ modulated at the frequency of the $Ar^+$ ions. Clearly, the transfer of the modulation from one species to another provides evidence for the reactions $Ar^+ + 2CH_4 \rightarrow Ar + CH_3^+ + H^\bullet + CH_4 \rightarrow Ar + C_2H_5^+ +$ neutrals.

Further work is in progress to explore the effects of laser pulses applied to the ions in the course of the reaction interval $\tau_m$ of the experiment. Such techniques open new perspectives for studying very complex reaction networks.

As mentioned above, the third pulse is normally chirped, so that the $\omega_2$ domain may extend over a large bandwidth. In some cases however, it may be of interest to use very high resolution in the $\omega_2$ domain in order to distinguish reaction products that have similar mass-to-charge ratios. We have carried out two-dimensional experiments where the first two pulses were chirped, while the third pulse was derived from a monochromatic rf carrier. The signal was observed with heterodyne detection to obtain high-resolution spectra in the $\omega_2$ domain. This allowed us to distinguish the product ions $CH_3D^{\bullet+}$ and $CH_5^+$, in order to identify the parent ions from which they originated. It does not seem worthwhile to provide illustrations of such spectra, for their general appearance is very similar to Figure 5.

### Experimental Section

The spectra were obtained with a Spectrospin CMS-47 FT-ICR spectrometer equipped with a 3 T superconducting magnet and an Aspect 3000 computer system. Methane ($CH_4$ and $CD_3H$, respectively) at $6.10^{-8}$ mbar was ionized with 20-ms pulses of 70-eV electrons. Other experimental conditions are given in the captions.

### Conclusions

We have shown that two-dimensional FT-ICR spectra can be obtained with frequency-swept pulses in order to overcome bandwidth limitations. Broad-band 2D FT-ICR appears to develop into a promising tool for investigating ion–molecule reactions and other processes such as photofragmentation. Frequency-swept pulses may also be useful in other applications of two-dimensional spectroscopy, such as in ESR spectra[8,9] and in rotational microwave spectra.[10] Whether two-dimensional techniques will prove to be competitive with traditional ion-ejection methods,[2,3] or with more elaborate schemes based on ion ejection such as the Hadamard method,[15] remains to be seen. Experience in NMR spectroscopy has shown that the appreciation of the relative merits of one- and two-dimensional spectroscopy may fluctuate as a result of the discovery of new methods and applications.[6]

**Acknowledgment.** We are indebted to A. G. Marshall, F. W. McLafferty and M. L. Gross for helpful comments. This research was supported in part by the Swiss National Science Foundation and by a grant from Spectrospin AG (Fällanden, Switzerland).

(15) McLafferty, F. W.; Stauffer, D. B.; Loh, S. Y.; Williams, E. R. *Anal. Chem.* **1987**, *59*, 2212.

# Unusual Spectroscopic Features in the Emission and Absorption Spectra of Single-Crystal $K_2[PtCl_4]$ Caused by Multiple-Mode Excited-State Distortions

**D. M. Preston,[†] Wolfgang Güntner,[‡] Alfred Lechner,[‡] Günter Gliemann,*[,‡] and Jeffrey I. Zink*[,†]**

*Contribution from the Department of Chemistry and Biochemistry, University of California, Los Angeles, California 90024-1569, and Institut für Physikalische und Theoretische Chemie, University of Regensburg, 8400 Regensburg, FRG.* *Received January 7, 1988*

**Abstract:** Two unusual features are observed in the electronic emission and absorption spectra of single-crystal $K_2[PtCl_4]$. First, a regularly spaced vibronic progression of 315 $cm^{-1}$ is observed in the luminescence spectrum which does not correspond to any normal vibrational modes of the molecule bound in the crystal. The spectrum is interpreted in terms of the missing mode effect (MIME). Calculations of the contributing vibrations and excited-state distortions are presented. Both the time-dependent theory and the eigenstate explanation are discussed. Second, a 1800-$cm^{-1}$ gap between the emission and absorption spectrum is found in which no measurable emission intensity or absorption intensity is observed. This energy gap is explained in terms of the intramolecular distortion along the non-totally symmetric mode which is required by the MIME. The magnitude of the energy gap is calculated from the distortion along this mode. The unmeasurable low vibronic intensities in the gap are explained by using the time-dependent theory of electronic spectroscopy.

The electronic emission and absorption spectra of the tetrachloroplatinate(II) ion and its derivatives are continuing to receive detailed attention.[1-6] In spite of the high symmetry and the apparent simplicity of the square-planar $PtCl_4^{2-}$, the electronic spectra and the electronic structure contain a number of interesting features.

[†] University of California, Los Angeles.
[‡] University of Regensburg.

(1) Martin, D. S.; Lenhardt, C. A. *Inorg. Chem.* **1964**, *3*, 1368.
(2) Martin, D. S.; Tucker, M. A.; Kassman, A. J. *Inorg. Chem.* **1965**, *4*, 1682.

0002-7863/88/1510-5628$01.50/0 